Int. J. Solids Structures Vol. 29, No. 14/15, pp. 1919–1937, 1992
Printed in Great Britain.

0020–7683/92 $5.00 + .00
Pergamon Press plc

DEVELOPMENT OF A MIXTURE MODEL FOR NONLINEAR WAVE PROPAGATION IN FIBER-REINFORCED COMPOSITES

H. MURAKAMI, T. J. IMPELLUSO and G. A. HEGEMIER
Department of Applied Mechanics and Engineering Sciences,
University of California at San Diego, La Jolla, CA 92093-0411, U.S.A.

Abstract—A method for constructing dispersive, nonlinear mixture models for unidirectionally fiber-reinforced composites is described. System nonlinearities in the treated example result from nonlinear material properties of the constituents. The proposed model is a nonlinear generalization of the linear model developed by Murakami and Hegemier [*Journal of Applied Mechanics*, Vol. 53, pp. 765–773 (1986)] for elastic constituents. Model construction is based upon a homogenization technique which employs multivariable asymptotic expansions in conjunction with certain weighted residual procedures. The methodology furnishes the equations of motion, the appropriate initial and boundary conditions, and a set of consistent rate constitutive relations. Model validation for linear and nonlinear dynamic responses is accomplished by comparing predicted results for wave-guide and wave-reflect problems with available experimental data or data obtained by use of a detailed finite element (FE) analysis. The validation studies reveal that the derived continuum model provides good simulations of complex wave phenomena and furnishes an economical alternative to detailed, explicit FE models. The studies performed reveal the importance of wave dispersion and attenuation phenomena in nonlinear as well as linear wave propagation in the composites.

INTRODUCTION

Composites are "designer" materials in the sense that a designer has the freedom to prescribe the material microstructure such that global response measures of interest are optimized for a given load environment together with certain cost/weight constraints. Such designer freedom, however, creates a need for material response models which are synthesized directly from material and geometrical information at the microstructural level. This need, in turn, stems from a desire to avoid a myriad of experiments which may be necessary to evaluate the material parameters associated with phenomenological models.

A situation of special interest to material designers concerns fiber-reinforced polymer and metal–matrix composites subject to dynamic load environments. Within the context of such materials and environments, response measures of stress wave attenuation and/or dispersion are often sought. For such problem types, one of the earliest successful attempts to synthesize a global response theory from microstructural information is due to Achenbach and Herrmann (1968) who formulated a higher-order continuum model, known as the "effective stiffness theory", to simulate elastic wave motion. Subsequent extensions and applications of this work were conducted by Bartholomew and Torvick (1972), Hlavacek (1975), Achenbach (1975, 1976), and Aboudi (1981). By modifying the original methodology Aboudi (1982, 1985) extended the linear model to account for viscoplastic material response. In parallel to the effective stiffness theories, attempts were made to develop mixture (multi-phase) continuum theories with microstructure. A representative cross-section of this subject includes the works by Martin *et al.* (1971), Choi and Bedford (1973), Hegemier *et al.* (1973), Hegemier and Gurtman (1974), Nayfeh (1977), Murakami *et al.* (1979), Nayfeh *et al.* (1984), and Murakami and Hegemier (1986).

To-date, the foregoing mixture theories have not been extended to model *nonlinear* material responses for *arbitrary* wave motion. In view of the potential modeling capability of the mixture descriptions, and in response to a perceived need, a procedure is illustrated in this paper for the mathematical construction of a higher-order mixture description of nonlinear wave propgation in unidirectional fiber-reinforced composites. The resulting model incorporates wave dispersion, wave attenuation, localized plastic flow, and effective

anisotropy. For clarity of presentation, the example construction treated herein is applied to a hexagonal array of fiber-reinforcement and rate-independent elastoplastic material nonlinearities. While the model construction procedure is applicable to arbitrary fiber layout, rate-dependent material response, and interfacial slip, extension and investigation of such cases are deferred to later publications.

The model construction method treated is based upon a multiscale homogenization technique developed by Hegemier and Gurtman (1974) for waveguide propagation and by Murakami and Hegemier (1986) for arbitrary linear wave motion. The methodology yields the equations of motion, the appropriate initial and boundary conditions, and a set of consistent rate constitutive relations. The derived continuum mixture theory is non-phenomenological in the sense that the model is synthesized from the composite "micro-structure" which consists of the fiber material and geometrical properties, the interface properties, and the matrix properties.

A considerable effort is made to validate the resulting model subsequent to its derivation. For this purpose, a numerical experiment is employed as the "exact" basis for comparison. Here numerical predictions from the continuum description are compared with detailed finite element (FE) results for several key time-dependent boundary value problems. This task necessitated the development of a special FE code for the model. The FE code DYNA2D (Hallquist, 1982) was employed to generate the "exact" reference data; for this purpose a fine mesh was used to explicitly model the composite microstructure.

In addition to information concerning accuracy, the validation calculations reveal some interesting features regarding response characteristics associated with wave dispersion, wave attenuation, localized plastic flow and effective anisotropy. These calculations also furnish enlightening information concerning computational efficiency.

FORMULATION

Consider a domain $\bar{V}$ with a uniaxial periodic array of fibers embedded in the matrix, as illustrated in Fig. 1. The position vector $\bar{\mathbf{x}}$ is described with respect to a rectangular Cartesian coordinate system $\bar{x}_i$, $i = 1$–3 with $\bar{x}_1$ in the axial direction of the fibers. In the $\bar{x}_2$, $\bar{x}_3$-plane, a typical cell that represents the geometrical microstructure of the composite is shown in Fig. 2 for a hexagonal array. For notational convenience forms $(\ )^{(\alpha)}$, $\alpha = 1, 2$ denote quantities associated with material α; here $\alpha = 1$ represents fiber and $\alpha = 2$ represents matrix. The notation $\bar{\nabla}$ is the gradient operator with respect to $\bar{\mathbf{x}}$ and $\dot{(\ )} = \partial(\ )/\partial \bar{t}$ will be employed in which $\bar{t}$ represents time. Furthermore, overbars will designate dimensional quantities; the lack of overbars will indicate nondimensional quantities.

The governing relations for the displacement vector $\bar{\mathbf{u}}$ $(=\bar{u}_i)$ and the stress tensor $\bar{\sigma}$ $(=\bar{\sigma}_{ij})$ in each material domain are as follows.

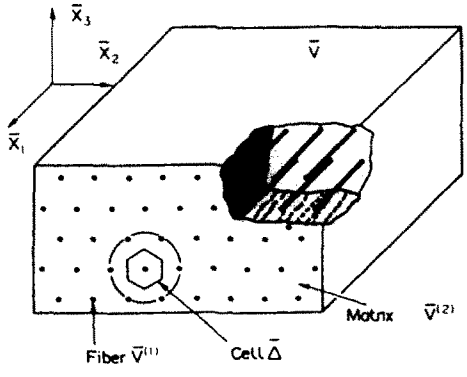

Fig. 1. A fiber-reinforced composite domain $\bar{V}$ with a uniaxial periodic array of fibers.

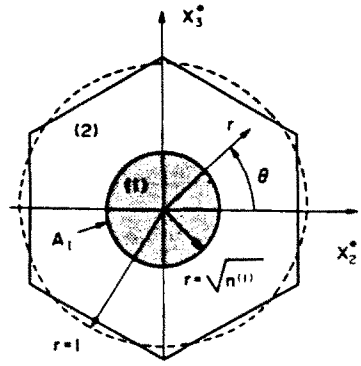

Fig. 2. A typical cell representing the geometric microstructure of the composite.

(a) Equations of motion:

$$\bar{\nabla}\cdot\bar{\boldsymbol{\sigma}}^{(\alpha)}+\bar{\mathbf{f}}^{(\alpha)}=\bar{\rho}^{(\alpha)}\ddot{\bar{\mathbf{u}}}^{(\alpha)},\quad \bar{\boldsymbol{\sigma}}^{(\alpha)}=\bar{\boldsymbol{\sigma}}^{(\alpha)\mathrm{T}}\quad \text{in } \bar{V}^{(\alpha)}, \tag{1}$$

where $\bar{\mathbf{f}}^{(\alpha)}$ $(=\bar{f}_i^{(\alpha)})$ is a constant body force, $\bar{\rho}^{(\alpha)}$ denotes mass density, and $(\ )^{\mathrm{T}}$ denotes transposition of the tensor $(\ )$.

(b) Rate constitutive relations:

$$\dot{\bar{\boldsymbol{\sigma}}}^{(\alpha)}=\bar{\mathbf{C}}^{(\alpha)(\mathrm{ep})}:\dot{\mathbf{e}}^{(\alpha)}(\mathbf{u}^{(\alpha)})\quad \text{in } \bar{V}^{(\alpha)} \tag{2}$$

$$\dot{\mathbf{e}}^{(\alpha)}(\bar{\mathbf{u}}^{(\alpha)})=\tfrac{1}{2}\{\bar{\nabla}\cdot\dot{\bar{\mathbf{u}}}^{(\alpha)}+(\bar{\nabla}\cdot\dot{\bar{\mathbf{u}}}^{(\alpha)})^{\mathrm{T}}\}\quad \text{in } \bar{V}^{(\alpha)}, \tag{3}$$

where $\dot{\mathbf{e}}^{(\alpha)}$ $(=\dot{e}_{ij}^{(\alpha)})$ is the rate of deformation under the small strain assumption, and $\bar{\mathbf{C}}^{(\mathrm{ep})}$ $(=\bar{C}_{ijkl}^{(\mathrm{ep})})$ is a tangent modulus tensor which becomes a constant tensor $\bar{\mathbf{C}}$ for elastic response.

(c) Interface continuity relations:

$$\bar{\mathbf{u}}^{(2)}-\bar{\mathbf{u}}^{(1)}=\mathbf{0},\quad \bar{\mathbf{v}}^{(1)}\cdot(\bar{\boldsymbol{\sigma}}^{(2)}-\bar{\boldsymbol{\sigma}}^{(1)})=\mathbf{0}\quad \text{on } \bar{A}_1, \tag{4}$$

where $\bar{A}_1$ is the interface between fiber and matrix, $\bar{\mathbf{v}}^{(1)}$ $(=\bar{v}_i^{(1)})$ denotes the outward normal on $\bar{A}_1$, and $\mathbf{0}$ is the zero vector.

(d) Displacement boundary data on $\partial\bar{V}_u$ and traction data on $\partial\bar{V}_T$ where $\partial\bar{V}=\partial\bar{V}_u\cup\partial\bar{V}_T$ is the boundary of $\bar{V}$.

(e) Initial conditions at $\bar{t}=0$.

In eqns (1)–(4), the Cartesian components of $\nabla\cdot\boldsymbol{\sigma}$, $\mathbf{C}:\dot{\mathbf{e}}$, and $\mathbf{v}\cdot\boldsymbol{\sigma}$ are $\sigma_{\mu j,j}$, $C_{ijkl}\dot{e}_{kl}$, and $v_j\sigma_{ji}$, respectively. The initial boundary value problem defined by the relations (a)–(e) on $\bar{V}=(\bar{V}^{(1)}\cup\bar{V}^{(2)})$ is well posed.

Most domains of practical interest contain a multitude of fibers; for such domains, a direct numerical finite element solution becomes intractable even with the use of supercomputers. In an effort to alleviate this problem, a higher-order continuum mixture model is developed to describe average measures of stress and deformation for both fiber and matrix, along with certain higher-order microstructural measures. This procedure was successfully applied to the elastic response of fiber-reinforced composites with a hexagonal array of fibers by Murakami and Hegemier (1986). In what follows, the above model is extended to include inelastic response of the constituents (eqn (2)).

MODEL DEVELOPMENT

Multivariable field representation

The derivation of the model commences with a scaling of both dependent and independent variables. To this end, it will be convenient to nondimensionalize the basic equations by using the following quantities (Hegemier and Gurtman, 1974):

$\bar{\Lambda}$	typical macrosignal wavelength
$\bar{\Delta}$	typical fiber spacing or cell dimension
$\bar{C}_{(m)}, \bar{\rho}_{(m)}$	reference wave velocity and macrodensity
$\bar{E}_{(m)} = \bar{\rho}_{(m)}\bar{C}^2_{(m)}$	reference modulus
$\bar{t}_{(m)} = \bar{\Lambda}/\bar{C}_{(m)}$	typical macrosignal travel time
$\varepsilon = \bar{\Delta}/\bar{\Lambda}$	ratio of micro-to-macrodimensions.

With the aid of the above notation, nondimensional variables are introduced according to:

$$(\mathbf{x}, \mathbf{u}^{(\alpha)}) = (\bar{\mathbf{x}}, \bar{\mathbf{u}}^{(\alpha)})/\bar{\Lambda}, \quad t = \bar{t}/\bar{t}_{(m)},$$
$$(\mathbf{C}, \boldsymbol{\sigma})^{(\alpha)} = (\bar{\mathbf{C}}, \bar{\boldsymbol{\sigma}})^{(\alpha)}/\bar{E}_{(m)}, \quad \rho^{(\alpha)} = \bar{\rho}^{(\alpha)}/\bar{\rho}_{(m)}. \tag{5}$$

The periodicity of both fiber array structure and material properties define a cell in the x_2, x_3-plane as shown in Fig. 2. The field variables in the composite exhibit significant variation over two length scales: the global and cell geometry. Further, an order of magnitude difference in the two length scales suggests the use of a multiscale or multivariable asymptotic technique (Babuska, 1976; Tartar, 1977; Bensoussan *et al.*, 1978; Hegemier *et al.*, 1979; Sanchez-Palencia, 1980; Murakami *et al.*, 1981). One introduces the microposition vector $\mathbf{x}^*$:

$$\mathbf{x}^* = \mathbf{x}/\varepsilon. \tag{6}$$

Field variables are now considered to be functions of both macro- and microposition vectors:

$$q^{(\alpha)}(\mathbf{x}, t) = \tilde{q}^{(\alpha)}(\mathbf{x}, \mathbf{x}^*, t; \varepsilon), \tag{7}$$

where $\mathbf{x} \in V$ and $\mathbf{x}^* \in A^{(\alpha)}$. The cell domain is heterogeneous in the $\mathbf{x}^*$-space and consists of $A^{(1)}$ and $A^{(2)}$ occupied by the fiber and matrix, respectively; the macrodomain V in the $\mathbf{x}$-space becomes homogeneous and is shared by the two constituents. Homogeneity of geometrical and material properties in the x_1-direction eliminates x_1^* dependence in eqn (7); heterogeneity is manifested only in the x_2, x_3-plane. Consequently, spatial derivatives take the new form:

$$\nabla q^{(\alpha)} = \nabla \tilde{q}^{(\alpha)} + \frac{1}{\varepsilon}\nabla^* \tilde{q}^{(\alpha)}, \tag{8}$$

where ∇^* is the gradient operator with respect to $\mathbf{x}^*$ and $(\ )_{,1^*} = \partial(\ )/\partial x_1^* = 0$. In the sequel $\tilde{q}$ will be written as q for notational simplicity.

The operations (7) and (8), when applied to all field variables nondimensionalized by eqn (5), lead to the following synthesized field equations.

(a) Equations of motion:

$$\nabla \cdot \boldsymbol{\sigma}^{(\alpha)} + \frac{1}{\varepsilon}\nabla^* \cdot \boldsymbol{\sigma}^{(\alpha)} + \mathbf{f}^{(\alpha)} = \rho^{(\alpha)}\ddot{\mathbf{u}}^{(\alpha)}, \quad \boldsymbol{\sigma}^{(\alpha)^T} = \boldsymbol{\sigma}^{(\alpha)} \quad \text{in } V \text{ and } A^{(\alpha)}. \tag{9}$$

(b) Rate constitutive relations:

$$\dot{\boldsymbol{\sigma}}^{(\alpha)} = \mathbf{C}^{(\alpha)(cp)} : \left\{\dot{\mathbf{e}}(\mathbf{u}^{(\alpha)}) + \frac{1}{\varepsilon}\dot{\mathbf{e}}^*(\mathbf{u}^{(\alpha)})\right\} \quad \text{in } V \text{ and } A^{(\alpha)}, \tag{10}$$

where

$$\dot{\mathbf{e}}(\mathbf{u}^{(\alpha)}) = \tfrac{1}{2}\{\nabla\dot{\mathbf{u}}^{(\alpha)} + (\nabla\dot{\mathbf{u}}^{(\alpha)})^{\mathrm{T}}\} \tag{11a}$$

$$\dot{\mathbf{e}}^{*}(\mathbf{u}^{(\alpha)}) = \tfrac{1}{2}\{\nabla^{*}\dot{\mathbf{u}}^{(\alpha)} + (\nabla^{*}\dot{\mathbf{u}}^{(\alpha)})^{\mathrm{T}}\}. \tag{11b}$$

(c) Interface continuity relations:

$$\mathbf{u}^{(2)} - \mathbf{u}^{(1)} = \mathbf{0}, \quad \boldsymbol{\nu}^{*(1)} \cdot (\boldsymbol{\sigma}^{(2)} - \boldsymbol{\sigma}^{(1)}) = \mathbf{0} \quad \text{on } A_{\mathrm{I}}, \tag{12}$$

where $\boldsymbol{\nu}^{*(1)}$ is a unit outward normal to $\mathbf{A}^{(1)}$.

(d) Displacement boundary data on ∂V_u and traction data on ∂V_{T}.

(e) Initial conditions at $t = 0$.

In eqns (9)–(11) it is understood that $(\ )_{,i^*} = 0$. The synthesized field variables (7) are now continuous with respect to $\mathbf{x}$ in V and may be piecewise continuous with respect to $\mathbf{x}^*$ in the cell due to the heterogeneity of the composite.

At this point, the field variables are assumed to satisfy a periodicity condition with respect to $\mathbf{x}^*$. According to this condition field variables take equal values on opposite sides of the cell boundary. Let the fundamental translation vectors of the periodic array in the x_2, x_3-plane be denoted by $\varepsilon\mathbf{d}_1$ and $\varepsilon\mathbf{d}_2$. In the x_2^*, x_3^*-plane $\mathbf{d}_1$ and $\mathbf{d}_2$ become the fundamental translation vectors (see for example, Kittel, 1971). Employing the direct notation $\mathbf{x} = (x_1, x_2, x_3)$, $\mathbf{x}^* = (0, x_2^*, x_3^*)$ the $\mathbf{x}^*$-periodicity condition for a general cell with the above fundamental translation vectors is expressed as

$$q(\mathbf{x}, \mathbf{x}^*, t) = q(\mathbf{x}, \mathbf{x}^* + m_1\mathbf{d}_1 + m_2\mathbf{d}_2, t), \tag{13}$$

where m_1 and m_2 assume the values ± 1 or 0.

The cell domain in the x_2^*, x_3^*-plane consists of subdomains $A^{(1)}$ and $A^{(2)}$. Let the volume (area) fraction of material α be denoted by $n^{(\alpha)}$; it satisfies

$$n^{(1)} + n^{(2)} = 1. \tag{14}$$

For a hexagonal array the actual cell may be modeled as two concentric cylinders (see Fig. 2) without significant loss of accuracy in dispersion spectra. For the concentric cylinders model the cell subdomains, $A^{(1)}$ and $A^{(2)}$, are represented as

$$A^{(1)} = \{(r, \theta) | 0 \leqslant r < \sqrt{n^{(1)}}, \quad 0 \leqslant \theta \leqslant 2\pi\} \tag{15a}$$

$$A^{(2)} = \{(r, \theta) | \sqrt{n^{(1)}} < r \leqslant 1, \quad 0 \leqslant \theta \leqslant 2\pi\}, \tag{15b}$$

where (r, θ) are polar coordinates defined in the x_2^*, x_3^*-plane such that

$$r = \sqrt{x_2^{*2} + x_3^{*2}}, \quad \tan\theta = x_3^*/x_2^*. \tag{15c}$$

For the concentric-cylinders model the cell boundary is denoted by $r = 1$ and the periodicity condition (13) simplifies as follows:

$$q(\mathbf{x}, r, \theta, t) = q(\mathbf{x}, r, \theta + \pi, t) \quad \text{on } r = 1. \tag{16}$$

When Fourier transforms are applied to both the spatial variable $\mathbf{x}$ and the time t, the $\mathbf{x}^*$-periodicity (13) takes the same form as the Floquet and Bloch theorems for harmonic wave in periodic structures (Brillouin, 1946; Kohn *et al.*, 1972). Although eqn (13) compromises the ability to capture microboundary layer effects on a cell-scale, it provides an economical means for predicting global boundary layer effects on a scale of down to a few cell lengths (Murakami, 1991), which is sufficient in most problems of interest.

Weighted residual procedure

In this subsection, a weighted residual procedure is introduced. This procedure will be subsequently used to eliminate $\mathbf{x}^*$ from all field variables through an averaging operation, and to establish appropriate equations of motion for the resulting average fields.

To begin, let $\psi^{(\alpha)}$, $\alpha = 1, 2$, denote the space of all $\mathbf{H}^1$-functions (see for example, Hughes, 1987) $q(\mathbf{x}, \mathbf{x}^*; t)$ on V with respect to $\mathbf{x}$ and on $A^{(\alpha)}$ with respect to $\mathbf{x}^*$ that are $\mathbf{x}^*$-periodic according to eqn (13). Functions $q^{(1)}$ and $q^{(2)}$ may suffer a discontinuity on the interface A_1. Any vector $\mathbf{u}^{(\alpha)}$ whose components $u_i^{(\alpha)} \in \psi^{(\alpha)}$ with $\mathbf{u}^{(\alpha)} = \hat{\mathbf{u}}^{(\alpha)}$ on $\partial V_u^{(\alpha)}$, where $\hat{\mathbf{u}}^{(\alpha)}$ is the specified boundary displacement vector, will be called an admissible trial displacement. Any function $\delta\mathbf{u}^{(\alpha)}$ whose components $\delta u_i^{(\alpha)} \in \psi^{(\alpha)}$ with $\delta\mathbf{u}^{(\alpha)} = \mathbf{0}$ on $\partial V_u^{(\alpha)}$ will be called a weighting function or an admissible variation of $u_i^{(\alpha)}$.

Next, consider the weighted residual R, defined by

$$\int_V \Bigg[\sum_{\alpha=1}^{2} \int_{A^{(\alpha)}} (\nabla \cdot \boldsymbol{\sigma}^{(\alpha)} + \frac{1}{\varepsilon} \nabla^* \cdot \boldsymbol{\sigma}^{(\alpha)} + \mathbf{f}^{(\alpha)} - \rho^{(\alpha)} \ddot{\mathbf{u}}^{(\alpha)}) \cdot \delta\mathbf{u}^{(\alpha)} \, dA^*$$

$$- \frac{1}{\varepsilon} \int_{\partial A} \boldsymbol{v}^{*(2)} \cdot \boldsymbol{\sigma}^{(2)} \cdot \delta\mathbf{u}^{(2)} \, ds^* + \frac{1}{\varepsilon} \int_{A_1} [\tfrac{1}{2} \boldsymbol{v}^{*(1)} \cdot (\boldsymbol{\sigma}^{(2)} - \boldsymbol{\sigma}^{(1)}) \cdot (\delta\mathbf{u}^{(1)} + \delta\mathbf{u}^{(2)})$$

$$+ \{\tfrac{1}{2} \boldsymbol{v}^{*(1)} \cdot (\boldsymbol{\sigma}^{(1)} + \boldsymbol{\sigma}^{(2)}) - \mathbf{T}^*\} \cdot (\delta\mathbf{u}^{(2)} - \delta\mathbf{u}^{(1)})] \, ds^* \Bigg] dV$$

$$+ \int_{\partial V_T} \Bigg\{ \sum_{\alpha=1}^{2} \int_{A^{(\alpha)}} ({}^{v}\mathbf{T}^{(\alpha)} - \boldsymbol{v} \cdot \boldsymbol{\sigma}^{(\alpha)}) \cdot \delta\mathbf{u}^{(\alpha)} \, dA^* \Bigg\} dA = R, \tag{17}$$

where $dV = dx_1 \, dx_2 \, dx_3$, $dA^* = dx_2^* \, dx_3^*$, ∂A is the cell boundary, ds^* is an infinitesimal line element, $\boldsymbol{v}^{*(2)}$ is a unit outward normal to $A^{(2)}$, and ${}^{v}\mathbf{T}^{(\alpha)}$ denotes the traction vector acting on an infinitesimal surface element dA with a unit outward normal $\boldsymbol{v}$ on ∂V_T. By virtue of the $\mathbf{x}^*$-periodicity the integrations with respect to macrocoordinates $\mathbf{x}$ are carried out over the entire domain V, while that with respect to the microcoordinates $\mathbf{x}^*$ is performed over the cell subdomain $A^{(\alpha)}$.

If $R = 0$ is satisfied for all admissible $\delta\mathbf{u}^{(\alpha)}$ which satisfy (13) and are arbitrary over V, on ∂V_T, and on $A^{(\alpha)}$, then it is evident that weak solutions of the local equations of motion (9) have been generated. These weak solutions then satisfy the traction boundary specified in (d) on ∂V_T and the traction continuity (12) on A_1.

From (17) with $R = 0$, Gauss' theorem, and the $\mathbf{x}^*$-periodicity condition (13), one obtains

$$\int_V \Bigg[\sum_{\alpha=1}^{2} \int_{A^{(\alpha)}} \Bigg\{ \Bigg(\delta\mathbf{e}^{(\alpha)} + \frac{1}{\varepsilon} \delta\mathbf{e}^{*(\alpha)} \Bigg) : \boldsymbol{\sigma}^{(\alpha)} - \delta\mathbf{u}^{(\alpha)} \cdot (\mathbf{f}^{(\alpha)} - \rho^{(\alpha)} \ddot{\mathbf{u}}^{(\alpha)}) \Bigg\} dA^*$$

$$+ \frac{1}{\varepsilon} \int_{A_1} (\delta\mathbf{u}^{(2)} - \delta\mathbf{u}^{(1)}) \cdot \mathbf{T}^* \, ds^* \Bigg] dV = \int_{\partial V_T} \Bigg\{ \sum_{\alpha=1}^{2} \int_{A^{(\alpha)}} \delta\mathbf{u}^{(\alpha)} \cdot {}^{v}\mathbf{T}^{(\alpha)} \, dA^* \Bigg\} dA, \tag{18}$$

where the components of $\delta\mathbf{e} : \boldsymbol{\sigma}$ are $\delta e_{ij} \sigma_{ij}$, and

$$\delta\mathbf{e}^{(\alpha)} = \tfrac{1}{2}\{\nabla\delta\mathbf{u}^{(\alpha)} + (\nabla\delta\mathbf{u}^{(\alpha)})^{\mathrm{T}}\}, \quad \delta\mathbf{e}^{*(\alpha)} = \tfrac{1}{2}\{\nabla^*\delta\mathbf{u}^{(\alpha)} + (\nabla^*\delta\mathbf{u}^{(\alpha)})^{\mathrm{T}}\}. \tag{19}$$

Equation (18) can be envisioned as the principle of virtual work for the synthesized fields. This principle furnishes a useful tool for generating the equations of motion associated with any order of continuum models.

Asymptotic analysis

In order to generate a continuum model from (18), the assumed $\mathbf{x}^*$-dependency of the displacement field must be described explicitly. The necessary microstructural information

for this operation was obtained for the elastic response of composites with a hexagonal array of fibers by an asymptotic procedure (Murakami and Hegemier, 1986). This procedure is based upon the premise that the typical cell length is much smaller than the macro-dimension, $\varepsilon \ll 1$. Therefore, the form of scaled eqns (9)–(12) suggests the expansion of the dependent variables in the asymptotic series (Lene and Leguillon, 1982):

$$\mathbf{u}^{(\alpha)}(\mathbf{x}, \mathbf{x}^*, t, \varepsilon) = \mathbf{u}^{(\alpha)}_{(0)}(\mathbf{x}, \mathbf{x}^*, t) + \varepsilon \mathbf{u}^{(\alpha)}_{(1)}(\mathbf{x}, \mathbf{x}^*, t) + \varepsilon^2 \mathbf{u}^{(\alpha)}_{(2)}(\mathbf{x}, \mathbf{x}^*, t) + \cdots \tag{20a}$$

$$\boldsymbol{\sigma}^{(\alpha)}(\mathbf{x}, \mathbf{x}^*, t, \varepsilon) = \frac{1}{\varepsilon} \boldsymbol{\sigma}^{(\alpha)}_{(-1)}(\mathbf{x}, \mathbf{x}^*, t) + \boldsymbol{\sigma}^{(\alpha)}_{(0)}(\mathbf{x}, \mathbf{x}^*, t) + \varepsilon \boldsymbol{\sigma}^{(\alpha)}_{(1)}(\mathbf{x}, \mathbf{x}^*, t) + \cdots \tag{20b}$$

$$\mathbf{C}^{(\alpha)(\mathrm{ep})} = \mathbf{C}^{(\alpha)(\mathrm{ep})}_{(0)} + \varepsilon \mathbf{C}^{(\alpha)(\mathrm{ep})}_{(1)} + \varepsilon^2 \mathbf{C}^{(\alpha)(\mathrm{ep})}_{(2)} + \cdots \tag{20c}$$

where $\mathbf{u}^{(\alpha)}_{(n)}$, $\boldsymbol{\sigma}^{(\alpha)}_{(n)}$ and $\mathbf{C}^{(\alpha)}_{(n)}$ satisfy the $\mathbf{x}^*$-periodicity condition. In the sequel, a class of hardening elastoplastic materials, which admit a rate potential and have a positive definite tangent modulus tensor, is considered. Consequently, $\mathbf{C}^{(\alpha)(\mathrm{ep})}_{(0)}$ is also assumed to be symmetric and positive definite in the expansion (20c); this obviously holds for elastic responses where only $\mathbf{C}^{(\alpha)(\mathrm{ep})}_{(0)} = \mathbf{C}^{(\alpha)}$ is required.

If eqn (20) is substituted into eqns (9)–(12) and the coefficients of different powers of ε are equated to zero, a sequence of microboundary value problems (MBVPs) defined on the cell is obtained. The first three sets of MBVPs for the coefficients of ε^{-2}, ε^{-1}, and ε^0 are defined in what follows.

MBVPs for $O(\varepsilon^{-2})$:

$$\nabla^* \cdot \boldsymbol{\sigma}^{(\alpha)}_{(-1)} = \mathbf{0} \quad \text{in } A^{(\alpha)} \tag{21a}$$

$$\dot{\boldsymbol{\sigma}}^{(\alpha)}_{(-1)} = \mathbf{C}^{(\alpha)(\mathrm{ep})}_{(0)} : \dot{\mathbf{e}}^*(\mathbf{u}^{(\alpha)}_{(0)}) \quad \text{in } A^{(\alpha)} \tag{21b}$$

$$\mathbf{u}^{(2)}_{(0)} - \mathbf{u}^{(1)}_{(0)} = \mathbf{0}, \quad \boldsymbol{\nu}^{*(1)} \cdot (\boldsymbol{\sigma}^{(2)}_{(-1)} - \boldsymbol{\sigma}^{(1)}_{(-1)}) = \mathbf{0} \quad \text{on } A_1. \tag{21c,d}$$

From eqns (21a,b) the operator for $\mathbf{u}^{(\alpha)}_{(0)}$ may be expressed as

$$\mathbf{L}(\dot{\mathbf{u}}^{(\alpha)}_{(0)}) \equiv \nabla^* \cdot \{\mathbf{C}^{(\alpha)(\mathrm{ep})}_{(0)} : \dot{\mathbf{e}}^*(\mathbf{u}^{(\alpha)}_{(0)})\} = \mathbf{0} \quad \text{in } A^{(\alpha)}. \tag{22}$$

A solution of the problem is $\mathbf{u}_{(0)}$ which is independent of $\mathbf{x}^*$:

$$\mathbf{u}^{(\alpha)}_{(0)} = \mathbf{u}_{(0)}(\mathbf{x}, t), \quad \mathbf{e}^*(\mathbf{u}_{(0)}) = \boldsymbol{\sigma}^{(\alpha)}_{(-1)} = \mathbf{0}. \tag{23}$$

MBVP for $O(\varepsilon^{-1})$:

$$\nabla^* \cdot \boldsymbol{\sigma}^{(\alpha)}_{(0)} = \mathbf{0} \quad \text{in } A^{(\alpha)} \tag{24a}$$

$$\dot{\boldsymbol{\sigma}}^{(\alpha)}_{(0)} = \mathbf{C}^{(\alpha)(\mathrm{ep})}_{(0)} : \{\dot{\mathbf{e}}(\mathbf{u}_{(0)}) + \dot{\mathbf{e}}^*(\mathbf{u}^{(\alpha)}_{(1)})\} \quad \text{in } A^{(\alpha)} \tag{24b}$$

$$\mathbf{u}^{(2)}_{(1)} - \mathbf{u}^{(1)}_{(1)} = \mathbf{0}, \quad \boldsymbol{\nu}^{*(1)} \cdot (\boldsymbol{\sigma}^{(2)}_{(0)} - \boldsymbol{\sigma}^{(1)}_{(0)}) = \mathbf{0} \quad \text{on } A_1. \tag{24c,d}$$

Equations (24a,b) imply that

$$\mathbf{L}(\dot{\mathbf{u}}^{(\alpha)}_{(1)}) \equiv \nabla^* \cdot \{\mathbf{C}^{(\alpha)(\mathrm{ep})}_{(0)} : \dot{\mathbf{e}}^*(\mathbf{u}^{(\alpha)}_{(1)})\} = -\nabla^* \cdot \{\mathbf{C}^{(\alpha)(\mathrm{ep})}_{(0)} : \dot{\mathbf{e}}(\mathbf{u}_{(0)})\}. \tag{25}$$

Equation (25) shows that $\mathbf{u}^{(\alpha)}_{(1)}$ is governed by the same operator as that of eqn (22) for $\mathbf{u}^{(\alpha)}_{(0)}$ except for the right-hand side. Even if the right-hand side of eqn (25) is nonzero it vanishes when integrated over the cell. As a result, the integrability condition for $\mathbf{u}^{(\alpha)}_{(1)}$ is satisfied. The form of the forcing term in eqn (25) suggests the following expression for $\mathbf{u}^{(\alpha)}_{(1)}$:

$$\dot{\mathbf{u}}^{(\alpha)}_{(1)}(\mathbf{x}, \mathbf{x}^*, t) = \dot{e}_{pq}(\mathbf{u}_{(0)}) \chi^{pq(\alpha)}(\mathbf{x}^*) \tag{26}$$

where χ^{pq} is $\mathbf{x}^*$-periodic. The substitution of (26) into (24) yields an MBVP for each χ^{pq};

this is continuous over the cell due to the perfect bond condition (12). These problems are defined up to a constant vector with respect to $\mathbf{x}^*$. This constant term may be included in $\mathbf{u}^{(\alpha)}_{(0)}(\mathbf{x}, t)$. Therefore, it is convenient to choose χ^{pq} such that its integration over the cell vanishes:

$$\sum_{\alpha=1}^{2} \int_{A^{(\alpha)}} \chi^{pq(\alpha)}\, dA^* = 0. \tag{27}$$

MBVP for $O(\varepsilon^0)$:

$$\nabla^* \cdot \boldsymbol{\sigma}^{(\alpha)}_{(1)} = \rho^{(\alpha)} \ddot{\mathbf{u}}_{(0)} - \mathbf{f}^{(\alpha)} - \nabla \cdot \boldsymbol{\sigma}^{(\alpha)}_{(0)} \quad \text{in } A^{(\alpha)} \tag{28a}$$

$$\dot{\boldsymbol{\sigma}}^{(\alpha)}_{(1)} = \mathbf{C}^{(\alpha)(\mathrm{ep})}_{(0)} : \{\dot{\mathbf{e}}(\mathbf{u}^{(\alpha)}_{(1)}) + \dot{\mathbf{e}}^*(\mathbf{u}^{(\alpha)}_{(2)})\} + \mathbf{C}^{(\alpha)(\mathrm{ep})}_{(1)} : \{\dot{\mathbf{e}}(\mathbf{u}_{(0)}) + \dot{\mathbf{e}}^*(\mathbf{u}^{(\alpha)}_{(1)})\} \quad \text{in } A^{(\alpha)} \tag{28b}$$

$$\mathbf{u}^{(2)}_{(2)} - \mathbf{u}^{(1)}_{(2)} = \mathbf{0}, \quad \boldsymbol{v}^{*(1)} \cdot (\boldsymbol{\sigma}^{(2)}_{(1)} - \boldsymbol{\sigma}^{(1)}_{(1)}) = \mathbf{0} \quad \text{on } A_1. \tag{28c,d}$$

At this point, it is instructive to outline the $O(1)$ homogenization procedure and to compare with the proposed $O(\varepsilon)$ homogenization procedure. Both homogenization procedures require the solution of the MBVPs for $\mathbf{u}^{(\alpha)}_{(1)}$ defined by eqns (24) and (26). The $O(1)$ equations of motion are obtained by imposing the integrability condition for $\mathbf{u}^{(\alpha)}_{(2)}$ on eqn (28a) without solving the MBVPs for $\mathbf{u}^{(\alpha)}_{(2)}$ (Bensoussan *et al.*, 1978; Sanchez-Palencia, 1980). According to the Fredholm alternative theorem, the problem defined in eqns (28) has a unique solution up to a constant vector with respect to $\mathbf{x}^*$, if the operator for $\mathbf{u}^{(\alpha)}_{(2)}$ in eqns (28) satisfies the integrability condition – the range of $\mathbf{L}(\mathbf{u}^{(\alpha)}_{(2)})$ is orthogonal to its kernel $\mathbf{u}^{(\alpha)}_{(0)} = \mathbf{u}_{(0)}(\mathbf{x}, t)$ (see for example, Marsden and Hughes, 1983). The same $O(1)$ equations of motion can be obtained by substituting the trial displacement field (31) in eqn (18) and by retaining only $O(1)$ terms. As a result, the $O(1)$ model neglects the kinetic energy associated with the $O(\varepsilon)$ displacement and fails to model harmonic wave dispersion. This deficiency is improved in the $O(\varepsilon)$ homogenization procedure.

Trial displacement and mixture equations of motion

The development of an $O(\varepsilon)$ homogenization commences with the definition of an average displacement field for each constituent, retaining terms up to and including $O(\varepsilon^2)$ terms:

$$\mathbf{U}^{(\alpha)}(\mathbf{x}, t) = \frac{1}{A^{(\alpha)}} \int_{A^{(\alpha)}} \{\mathbf{u}_{(0)} + \varepsilon \mathbf{u}^{(\alpha)}_{(1)} + \varepsilon^2 \mathbf{u}^{(\alpha)}_{(2)}\}\, dA^*, \tag{29}$$

where $A^{(\alpha)}$ denotes the cell subdomain for integration and the area for algebraic operations.

Equation (25) shows that $\mathbf{u}^{(\alpha)}_{(1)}$ is excited by $u_{p(0),q} + u_{q(0),p}$. Therefore, the mixture formulation becomes more tractable by introducing generalized displacement variables (parameters) which represent $u_{p(0),q} + u_{q(0),p}$, such that

$$S_{pq}(\mathbf{x}, t) = S_{qp} = \frac{1}{\varepsilon A} \int_{A_1} \mathbf{u}^{(\alpha)} \cdot \boldsymbol{v}^{*(1)}\, ds^* \approx \frac{1}{A} \int_{A_1} \mathbf{u}^{(\alpha)}_{(1)} \cdot \boldsymbol{v}^{*(1)}\, ds^*, \tag{30}$$

where $A = A^{(1)} + A^{(2)}$ denotes the total area of the cell.

This yields the following trial displacement field

$$\mathbf{u}^{(\alpha)}(\mathbf{x}, \mathbf{x}^*, t; \varepsilon) \approx \mathbf{U}^{(\alpha)}(\mathbf{x}, t) + \varepsilon S_{pq}(\mathbf{x}, t) \chi^{pq(\alpha)}(\mathbf{x}^*). \tag{31}$$

In eqn (31) $\mathbf{U}^{(\alpha)}$ is the average displacement associated with each constituent, while $S_{pq}(\mathbf{x}, t)$ is the generalized displacement which represents the amplitude of the $O(\varepsilon)$ displacement microstructure. In the sequel, equation (31) will be used to obtain mixture equations of motion from eqn (18).

In order to find the $O(\varepsilon)$ displacement microstructure $\chi^{pq}(\mathbf{x}^*)$ one must solve six MBVPs defined by eqns (24) and (26). These problems were solved analytically by Murakami and Hegemier (1986) for a hexagonal cell, consisting of elastic constituents, approximated by the concentric-cylinders model. The exact solution indicates a good approximation for the $O(\varepsilon)$ displacements, and the following trial displacement field (in component form) was constructed for hexagonal cells:

$$u_i^{(\alpha)}(\mathbf{x}, \mathbf{x}^*, t, \varepsilon) \approx U_i^{(\alpha)}(\mathbf{x}, t) + \varepsilon[S_{i2}(\mathbf{x}, t)\cos\theta + S_{i3}(\mathbf{x}, t)\sin\theta]g^{(\alpha)}(r), \tag{32a}$$

where

$$g^{(\alpha)}(r) = (-1)^{\alpha+1}\frac{1}{n^{(\alpha)}}\left(r - \delta_{\alpha 2}\frac{1}{r}\right) \tag{32b}$$

$$S_{23} = S_{32}, \tag{32c}$$

and where $\delta_{\alpha\beta}$ is the Kronecker delta. The generalized displacements S_{ij} are not displacement components but parameters; it is convenient to employ the component form in eqns (32). The functions $g^{(\alpha)}(r)\cos\theta$ and $g^{(\alpha)}(r)\sin\theta$ are the approximations for χ^{pq} and satisfy the $\mathbf{x}^*$-periodicity condition (16) and the normalization condition (27). The effectiveness of the above trial displacements to simulate harmonic wave dispersion was demonstrated for hexagonal and square arrays in the above reference. For arbitrary cells and elastic constituents one can numerically solve the MBVPs for χ^{pq} by finite element methods and numerically construct approximate solutions. *These approximate solutions are functions of* $\mathbf{x}^*$ *and are independent of material properties; therefore they apply to both isotropic and orthotropic constituents.*

For nonlinear responses χ^{pq} can be found by solving the rate-MBVPs since the tangent moduli must be evaluated for each $\dot{\mathbf{e}}(\mathbf{u}_{(0)})$; this implies that χ^{pq} differs for each load increment. To render the following analysis tractable, an approximate solution for χ^{pq} which is independent of the load increment was constructed. *By virtue of very weak anisotropy introduced to the nonzero and off-diagonal entries of the elastic modulus tensor, it is found that the approximate* χ^{pq} *for elastic response furnishes a good approximation even for elastoplastic deformation.* This situation is similar to the nonlinear plate and shell analyses in which a linear variation of the in-plane displacements over the thickness of the plate and shell—found for elastic responses—yields a good approximation even for nonlinear response. The soundness of the above approximation will be examined in the sequel by comparing the model prediction with one obtained via a detailed finite element analysis. In what follows, the above theory will be applied to a hexagonal cell with the concentric-cylinders approximation.

Substitution of eqns (32) into eqn (18) yields the mixture equations of motion and associated boundary conditions together with the inherited initial conditions; they are given in component form as follows.

(a) Mixture equations of motion:

$$n^{(\alpha)}\sigma_{ji,j}^{(\alpha a)} + (-1)^{\alpha+1}P_i + n^{(\alpha)}f_i^{(\alpha)} = n^{(\alpha)}\rho^{(\alpha)}\ddot{U}_i^{(\alpha)} \tag{33}$$

$$\overset{2}{M}_{ji,j} + \frac{1}{\varepsilon^2}(\sigma_{2i}^{(2a)} - \sigma_{2i}^{(1a)} + R_{2i}) = I\ddot{S}_{i2}, \quad i = 1, 2 \tag{34a}$$

$$\overset{3}{M}_{ji,j} + \frac{1}{\varepsilon^2}(\sigma_{3i}^{(2a)} - \sigma_{3i}^{(1a)} + R_{3i}) = I\ddot{S}_{i3}, \quad i = 1, 3 \tag{34b}$$

$$\tfrac{1}{2}(\overset{3}{M}_{j2,j} + \overset{2}{M}_{j3,j}) + \frac{1}{\varepsilon^2}(\sigma_{23}^{(2a)} - \sigma_{23}^{(1a)} + R_{23}) = I\ddot{S}_{23}, \tag{34c}$$

where the average operations are defined by

$$\sigma_{ij}^{(\alpha)}(\mathbf{x}, t) = \frac{1}{A^{(\alpha)}} \int_{A^{(\alpha)}} \sigma_{ij}^{(\alpha)}(\mathbf{x}, \mathbf{x}^*, t)\, \mathrm{d}A^* \tag{35}$$

$$P_i(\mathbf{x}, t) = \frac{1}{\varepsilon A} \int_{A_1} \sigma_{\mu}^{(\alpha)} v_{\nu}^{(1)}\, \mathrm{d}s^* \approx \frac{1}{A} \int_{A_1} \sigma_{\mu(1)}^{(\alpha)} v_{\nu}^{(1)}\, \mathrm{d}s^* \tag{36}$$

$$\varepsilon(\overset{2}{M}_{ij}, \overset{3}{M}_{ij}) = \frac{1}{A} \sum_{\alpha=1}^{2} \int_{A^{(\alpha)}} \sigma_{ij}^{(\alpha)} g^{(\alpha)}(\cos\theta, \sin\theta)\, \mathrm{d}A^* \tag{37}$$

$$R_{2i} = \frac{1}{n^{(2)} A} \int_{A^{(2)}} \frac{1}{r^2} (\sigma_{2i}^{(2)} \cos 2\theta + \sigma_{3i}^{(2)} \sin 2\theta)\, \mathrm{d}A^*, \quad i = 1, 2 \tag{38a}$$

$$R_{3i} = \frac{1}{n^{(2)} A} \int_{A^{(2)}} \frac{1}{r^2} (-\sigma_{3i}^{(2)} \cos 2\theta + \sigma_{2i}^{(2)} \sin 2\theta)\, \mathrm{d}A^*, \quad i = 1, 3 \tag{38b}$$

$$R_{23} = \frac{1}{n^{(2)} A} \int_{A^{(2)}} \frac{1}{2r^2} (\sigma_{22}^{(2)} + \sigma_{33}^{(2)}) \sin 2\theta\, \mathrm{d}A^* \tag{38c}$$

$$\mathrm{I} = \sum_{\alpha=1}^{2} h^{(\alpha)} \rho^{(\alpha)}, \quad h^{(1)} = \tfrac{1}{4}, \quad h^{(2)} = -\frac{1}{4n^{(2)}} \left(2 + n^{(2)} + \frac{2}{n^{(2)}} \ln n^{(1)}\right). \tag{39}$$

In eqns (36)–(38) A ($=\pi$) denotes the area of the cell.

(b) Boundary conditions:

$$U_i^{(\alpha)} \quad \text{or} \quad n^{(\alpha)} \sigma_{\mu}^{(\alpha)} v_{\nu} \quad \text{specified for } i = 1\text{–}3 \tag{40}$$

$$S_{i2} \quad \text{or} \quad \overset{2}{M}_{\mu} v_{\nu} \quad \text{specified for } i = 1, 2 \tag{41a}$$

$$S_{i3} \quad \text{or} \quad \overset{3}{M}_{\mu} v_{\nu} \quad \text{specified for } i = 1, 3 \tag{41b}$$

$$S_{23} \quad \text{or} \quad (\overset{3}{M}_{\beta 2} + \overset{2}{M}_{\beta 3}) v_{\nu} \quad \text{specified.} \tag{41c}$$

(c) Initial conditions:

$$U_i^{(\alpha)}, \dot{U}_i^{(\alpha)}, S_{i2}, S_{i3}, \dot{S}_{i2}, \dot{S}_{i3} \quad \text{specified at } t = 0. \tag{42}$$

It is noted here that the above mixture equations are identical to those for elastic constituents (Murakami and Hegemier, 1986).

Incremental constitutive relations and trial transverse stress-rate

At first glance, it would appear that the trial displacements (32) could be used together with the original three-dimensional material constitutive relations (10) and the stress-type averages (35)–(38) to establish a set of constitutive equations for the stress averages to accompany the equations of motion (33) and (34). A closer examination, however, reveals that such an approach will not yield a relation for the interaction body force **P** in (36) and will lead to a model which is too "stiff" and which exhibits erroneous dispersive characteristics. These problems—common to the use of direct variational methods—can be alleviated by the use of a judicious mixed weighted residual procedure wherein the trial functions include certain stress-rate components as well as the velocity components. Such a procedure is an incremental version of Reissner's mixed variational principle (Reissner, 1984, 1986) which was employed to derive the mixture model for elastic constituents (Murakami and Hegemier, 1986).

In order to use the mixed weighted residual procedure, it is necessary to rewrite the rate constitutive relations (10) in terms of in-plane strain rates and transverse stress rates; these are shown in matrix form for easy finite element implementation:

$$\dot{\sigma}_{11} = E_{11}\dot{e}_{11} + [E_{12}]\{\dot{\sigma}_t\} \tag{43a}$$

$$\{\dot{e}_t\} = -[E_{12}]^T\dot{e}_{11} + [E_{22}]\{\dot{\sigma}_t\}, \tag{43b}$$

where

$$\{\sigma_t\} = [\sigma_{22} \quad \sigma_{33} \quad \sigma_{23} \quad \sigma_{31} \quad \sigma_{12}]^T,$$

$$\{e_t\} = [e_{22} \quad e_{33} \quad 2e_{23} \quad 2e_{31} \quad 2e_{12}]^T + \frac{1}{\varepsilon}[e^*_{22} \quad e^*_{33} \quad 2e^*_{23} \quad 2e^*_{31} \quad 2e^*_{12}]^T. \tag{44}$$

In eqns (43) and (44) $[\ ]^T$ is the transposition of $[\ ]$; subscript t denotes transverse quantities. The transverse stresses are those which appear in the traction continuity condition (12b), i.e. all stress components except $\sigma^{(\alpha)}_{11}$. The matrices $[E_{ij}]$ are functions of the elements of $C^{(ep)}_{ijkl}$ and $[E^{(\alpha)}_{22}]$ is symmetric and positive definite for hardening materials. Specific forms of $[E^{(\alpha)}_{ij}]$ employed for the numerical study are given in the Appendix and obtained for the von Mises yield criterion and associative flow rule with isotropic strain hardening.

Let $\dot{\psi}^{(\alpha)}$ ($\alpha = 1, 2$) denote the space of all $\mathbf{H}^1$-functions $\dot{q}(\mathbf{x}, \mathbf{x}^*, t)$ on V with respect to $\mathbf{x}$ and on $A^{(\alpha)}$ with respect to $\mathbf{x}^*$ that are $\mathbf{x}^*$-periodic according to eqn (13). Functions $\dot{q}^{(1)}$ and $\dot{q}^{(2)}$ may suffer a discontinuity on the interface A_I. Any vector $\dot{\mathbf{u}}^{(\alpha)}$ whose components belong to $\dot{\psi}^{(\alpha)}$ with $\dot{\mathbf{u}}^{(\alpha)} = \dot{\hat{\mathbf{u}}}^{(\alpha)}$ on $\partial V^{(\alpha)}_u$, where $\dot{\hat{\mathbf{u}}}^{(\alpha)}$ is the specified boundary velocity, will be called an admissible trial velocity. Any function $\delta\dot{\mathbf{u}}^{(\alpha)}$ whose components belong to $\dot{\psi}^{(\alpha)}$ with $\delta\dot{\mathbf{u}}^{(\alpha)} = \mathbf{0}$ on $\partial V^{(\alpha)}_u$ will be called a weighting function. The space of admissible transverse stress-rate $\{\dot{\sigma}^{(\alpha)}_t\}$ ($\alpha = 1, 2$) consists of all $\mathbf{H}^0$ ($= \mathbf{L}_2$) functions $\dot{q}(\mathbf{x}, \mathbf{x}^*, t)$ on V with respect to $\mathbf{x}$ and on $A^{(\alpha)}$ with respect to $\mathbf{x}^*$ that are $\mathbf{x}^*$-periodic. The mixed weighted residual procedure applied to the rate boundary value problem defined by (9)–(12) yields in matrix form:

$$\int_V \Bigg[\sum_{\alpha=1}^{2} \int_{A^{(\alpha)}} \{\delta\dot{e}^{(\alpha)}_{11}\dot{\sigma}^{(\alpha)}_{11} + \{\delta\dot{e}^{(\alpha)}_t\}^T\{\dot{\sigma}^{(\alpha)}_t\} + \{\delta\dot{u}^{(\alpha)}\}^T\{\rho\dot{a}^{(\alpha)}\}$$

$$+ \delta\{\dot{\sigma}^{(\alpha)}_t\}^T(\{\dot{e}^{(\alpha)}_t\} + [E^{(\alpha)}_{12}]^T\dot{e}^{(\alpha)}_{11} - [E^{(\alpha)}_{22}]\{\dot{\sigma}^{(\alpha)}_t\})\} \, dA^*$$

$$+ \frac{1}{\varepsilon}\int_{A_I} [(\{\delta\dot{u}^{(2)}\}^T - \{\delta\dot{u}^{(1)}\}^T)\{\dot{T}^*\} + \{\delta\dot{T}^*\}^T(\{\dot{u}^{(2)}\} - \{\dot{u}^{(1)}\})] \, ds^* \Bigg] dV$$

$$= \int_{\partial V_T} \Bigg[\sum_{\alpha=1}^{2} \int_{A^{(\alpha)}} \{\delta\dot{u}^{(\alpha)}\}^T\{{}^v\dot{T}^{(\alpha)}\} \, dA^* \Bigg] dA, \tag{45}$$

where $\{\delta\dot{u}\}$, $\{\rho a\}$, $\{T^*\}$, and $\{{}^vT\}$ are, respectively, the matrix representation of $\delta\dot{\mathbf{u}}$, $\rho\ddot{\mathbf{u}}$, $\mathbf{T}^*$, and ${}^v\mathbf{T}$.

For arbitrary variation of $\{\dot{u}^{(\alpha)}\}$ and $\{\dot{\sigma}^{(\alpha)}_t\}$, one obtains the rate constitutive relation for $\{\dot{e}^{(\alpha)}_t\}$ in (43b), as well as the rate equations of motion (9), the rate boundary conditions (d), and the rate form of eqn (12). Equation (43a) is considered to be the definition of $\dot{\sigma}^{(\alpha)}_{11}$. The mixed weighted residual equation (45) with appropriate trial functions for $\{\dot{u}^{(\alpha)}\}$ ($= \dot{\mathbf{u}}^{(\alpha)}$) and $\{\dot{\sigma}^{(\alpha)}_t\}$ yields the rate constitutive relations for the stress averages in eqns (35)–(38). The rate form of (32a) furnishes a trial velocity field. The trial transverse stress rate has the form

$$\{\dot{\sigma}^{(\alpha)}_t\} \approx \{\dot{\sigma}^{(\alpha)}_{t(0)}\}(\mathbf{x}, \mathbf{x}^*, t) + \varepsilon\{\dot{\sigma}^{(\alpha)}_{t(1)}\}(\mathbf{x}, \mathbf{x}^*, t). \tag{46}$$

In accordance with the $O(1)$ homogenization procedure, the $O(1)$ transverse stress-rate $\{\dot{\sigma}_{t(0)}\}$ can be constructed by using the approximate velocity field defined from eqn (31). Accordingly, for a hexagonal array, substitution of the trial velocity field obtained from (32) into (10) furnishes the following form for the transverse stress-rate:

$$\{\dot{\sigma}^{(\alpha)}_{(0)}\} \approx \{\dot{\tau}^{(\alpha)}\}(\mathbf{x}, t) + \delta_{\alpha 2}\frac{1}{r^2}[T(\theta)]\{\dot{t}_1\}(\mathbf{x}, t), \tag{47a}$$

where $\{\tau^{(\alpha)}\}$ and $\{t_1\}$ are stress variables defined as

$$\{\tau^{(\alpha)}\}(\mathbf{x}, t) = [\tau^{(\alpha)}_{22} \quad \tau^{(\alpha)}_{33} \quad \tau^{(\alpha)}_{23} \quad \tau^{(\alpha)}_{31} \quad \tau^{(\alpha)}_{12}]^{\mathrm{T}} \tag{47b}$$

$$\{t_1\}(\mathbf{x}, t) = [t_{22} \quad t_{33} \quad t_{23} \quad t_{31} \quad t_{12}]^{\mathrm{T}}, \tag{47c}$$

and where $[T(\theta)]$ is a 5×5 matrix whose nonzero elements are

$$\begin{aligned} T_{11} = T_{12} = T_{21} = -T_{22} = T_{44} = T_{55} = \cos 2\theta \\ T_{13} = T_{23} = T_{32} = T_{45} = -T_{54} = \sin 2\theta. \end{aligned} \tag{47d}$$

The $O(\varepsilon)$ term $\{\sigma^{(\alpha)}_{(1)}\}$ is governed by the MBVP (28) which requires the solution of $\mathbf{u}^{(\alpha)}_{(2)}$. The exact analysis of $\mathbf{u}^{(\alpha)}_{(2)}$ based upon the expansion (20a) and eqns (23) and (26) yields 42 sub-MBVPs. The formidable task of solving for the elements of $\mathbf{u}^{(\alpha)}_{(2)}$ can be alleviated by constructing $\{\sigma^{(\alpha)}_{(1)}\}$ approximately from (28a). Examination of the analytical solutions for a concentric-cylinders cell reveals that $\{\sigma^{(\alpha)}_{(1)}\}$, which satisfies

$$\nabla^* \cdot \dot{\boldsymbol{\sigma}}^{(\alpha)}_{(1)} = (-1)^{\alpha+1}\dot{\mathbf{P}}/n^{(\alpha)} \quad \text{in } A^{(\alpha)}, \tag{48}$$

yields a simple approximation for a general cell.

Equation (48) is obtained by applying the Gauss theorem to eqn (36) and satisfies the integrability condition for $\mathbf{u}^{(\alpha)}_{(2)}$ through the explicit introduction of $\mathbf{P}$. For a hexagonal cell the following approximation (adopted for elastic constituents) is employed

$$\{\dot{\sigma}^{(\alpha)}_{(1)}\} \approx \tfrac{1}{4}g^{(\alpha)}(r)[Q(\theta)]\{\dot{P}\}(\mathbf{x}, t), \tag{49a}$$

where $\{P\}$ is a matrix representation of $\mathbf{P}$, and $[Q(\theta)]$ is a 5×3 matrix whose nonzero elements are

$$\begin{aligned} Q_{22} = Q_{33} = \tfrac{1}{3}Q_{12} = \tfrac{1}{2}Q_{51} = \cos\theta \\ Q_{13} = Q_{32} = \tfrac{1}{3}Q_{23} = \tfrac{1}{2}Q_{41} = \sin\theta. \end{aligned} \tag{49b}$$

The trial transverse stress-rate is now obtained by substituting eqns (47) and (49) into eqn (46).

On substituting the rate form of eqn (32) and eqn (46) into eqn (45), one obtains the rate form of (33), (34), (40) and (41). In addition, the arbitrary variation of $\{\dot{\sigma}^{(\alpha)}_1\}$ yields the rate constitutive relations for the transverse stress variables:

$$\int_{A^{(\alpha)}} [E^{(\alpha)}_{22}]\left(\{\dot{\tau}^{(\alpha)}\} + \delta_{\alpha 2}\frac{1}{r^2}[T]\{\dot{t}_1\} + \frac{\varepsilon}{4}g^{(\alpha)}[Q]\{\dot{P}\}\right) \mathrm{d}A^* = n^{(\alpha)}\pi\left(\{\dot{e}^{(\alpha)}_{(0)}\} + (-1)^{\alpha+1}\frac{1}{n^{(\alpha)}}\{\dot{S}\}\right) + \int_{A^{(\alpha)}} [E^{(\alpha)}_{12}]^{\mathrm{T}}\dot{e}^{(\alpha)}_{11}\,\mathrm{d}A^* \tag{50}$$

$$\int_{A^{(2)}} \frac{1}{r^2}[T]^{\mathrm{T}}[E^{(2)}_{22}]\left(\{\dot{\tau}^{(2)}\} + \frac{1}{r^2}[T]\{\dot{t}_1\} + \frac{\varepsilon}{4}g^{(2)}[Q]\{\dot{P}\}\right) \mathrm{d}A^* = \pi[W]\{\dot{S}\} + \int_{A^{(2)}} \frac{1}{r^2}[T]^{\mathrm{T}}[E^{(2)}_{12}]^{\mathrm{T}}\dot{e}^{(2)}_{11}\,\mathrm{d}A^* \tag{51}$$

$$\frac{\varepsilon}{4}\sum_{\alpha=1}^{2}\int_{A^{(\alpha)}} g^{(\alpha)}[Q]^{\mathrm{T}}[E_{22}^{(\alpha)}]\left(\{\dot{\tau}^{(\alpha)}\}+\delta_{\alpha 2}\frac{1}{r^2}[T]\{\dot{t}_1\}+\frac{\varepsilon}{4}g^{(\alpha)}[Q]\{\dot{P}\}\right)\mathrm{d}A^*$$

$$=\pi(\{\dot{U}^{(2)}\}-\{\dot{U}^{(1)}\})+\pi\frac{\varepsilon^2 h}{4}([R^{\mathrm{I}}]\{\dot{S}\}_{,1}+[R^{\mathrm{II}}]\{\dot{S}\}_{,2}+[R^{\mathrm{III}}]\{\dot{S}\}_{,3})$$

$$+\frac{\varepsilon}{4}\sum_{\alpha=1}^{2}\int_{A^{(\alpha)}} g^{(\alpha)}[Q]^{\mathrm{T}}[E_{12}^{(\alpha)}]^{\mathrm{T}}\dot{e}_{11}^{(\alpha)}\,\mathrm{d}A^*, \quad (52)$$

where $\{U^{(\alpha)}\}$ is a matrix representation of $\mathbf{U}^{(\alpha)}$, $h=h^{(1)}+h^{(2)}$, and

$$\{e_{(U)}^{(\alpha)}\}=[U_{2,2}^{(\alpha)}\quad U_{3,3}^{(\alpha)}\quad U_{2,3}^{(\alpha)}+U_{3,2}^{(\alpha)}\quad U_{3,1}^{(\alpha)}+U_{1,3}^{(\alpha)}\quad U_{1,2}^{(\alpha)}+U_{2,1}^{(\alpha)}]^{\mathrm{T}}$$

$$\{S\}=[S_{22}\quad S_{33}\quad 2S_{23}\quad S_{13}\quad S_{12}]^{\mathrm{T}}. \quad (53)$$

In eqns (50)–(52), $[W]$ is a 5×5 matrix, and $[R^{\mathrm{I}}]$, $[R^{\mathrm{II}}]$, $[R^{\mathrm{III}}]$ are 3×5 matrices. Nonzero elements of the latter matrices are

$$W_{11}=-W_{12}=W_{33}=-\frac{1}{2n^{(1)}},\quad W_{21}=W_{22}=-W_{44}=W_{55}=\frac{1}{n^{(1)}}$$

$$R_{11}^{\mathrm{I}}=R_{12}^{\mathrm{I}}=R_{15}^{\mathrm{II}}=R_{14}^{\mathrm{III}}=2,\quad R_{21}^{\mathrm{II}}=R_{32}^{\mathrm{III}}=3,\quad R_{22}^{\mathrm{II}}=R_{33}^{\mathrm{II}}=R_{31}^{\mathrm{III}}=R_{23}^{\mathrm{III}}=1. \quad (54)$$

The solution of (50), (51) and (52) yields $\{\dot{\tau}^{(\alpha)}\}$, $\{\dot{t}_1\}$, and $\{\dot{P}\}$ in terms of $\{\dot{e}_{(U)}^{(\alpha)}\}$, $\{\dot{S}\}$, $\dot{e}_{11}^{(\alpha)}$, and $\{\dot{U}^{(2)}\}-\{\dot{U}^{(1)}\}$. For inelastic response the integrals in (50)–(52) must be evaluated numerically at each increment (time step); for elastic constituents the above relations can be evaluated explicitly and this produces the results obtained from a fully elastic approach to the problem (Murakami and Hegemier, 1986). Substituting eqn (46) into eqns (37) and (38) one finds

$$\overset{2}{M}_{22}=3hP_2/4,\quad \overset{2}{M}_{13}=\overset{3}{M}_{23}=hP_2/4,\quad \overset{3}{M}_{33}=3hP_3/4,$$

$$\overset{2}{M}_{12}=\overset{3}{M}_{31}=hP_1/2,\quad \overset{3}{M}_{22}=\overset{2}{M}_{23}=hP_3/4,\quad \overset{2}{M}_{31}=\overset{3}{M}_{12}=0 \quad (55)$$

$$R_{21}=t_{12}/n^{(1)},\quad R_{22}=(t_{22}/2+t_{33})/n^{(1)},\quad R_{31}=-t_{31}/n^{(1)},$$

$$R_{23}=t_{23}/2n^{(1)},\quad R_{33}=(-t_{22}/2+t_{33})/n^{(1)}. \quad (56)$$

The remaining constitutive equations for $\dot{\sigma}_{11}^{(\alpha)}$ and $\dot{M}_{11}$ are obtained from eqns (43a), (35) and (37). The results are

$$n^{(\alpha)}\pi\dot{\sigma}_{11}^{(\alpha)}=\int_{A^{(\alpha)}}\left\{E_{11}^{(\alpha)}\dot{e}_{11}^{(\alpha)}+[E_{12}^{(\alpha)}]\left(\{\dot{\tau}^{(\alpha)}\}+\delta_{\alpha 2}\frac{1}{r^2}[T]\{\dot{t}_1\}+\frac{\varepsilon}{4}g^{(\alpha)}[Q]\{\dot{P}\}\right)\right\}\mathrm{d}A^* \quad (57)$$

$$\varepsilon\pi\{\dot{M}_p\}=\sum_{\alpha=1}^{2}\int_{A^{(\alpha)}} g^{(\alpha)}\{n\}\left[E_{11}^{(\alpha)}\dot{e}_{11}^{(\alpha)}+[E_{12}^{(\alpha)}]\left(\{\dot{\tau}^{(\alpha)}\}+\delta_{\alpha 2}\frac{1}{r^2}[T]\{\dot{t}_1\}+\frac{\varepsilon}{4}g^{(\alpha)}[Q]\{\dot{P}\}\right)\right]\mathrm{d}A^*, \quad (58a)$$

where

$$\{M_p\}=[\overset{2}{M}_{11}\quad \overset{3}{M}_{11}]^{\mathrm{T}},\quad \{n\}=[\cos\theta\quad \sin\theta]^{\mathrm{T}}. \quad (58b)$$

The above operations were carried out at each integration point in a constitutive subroutine for the mixture finite element code: HFEC2D (Impelluso, 1990).

Table 1. Material properties for wave-reflect problem

Material α	Volume fraction $n^{(\alpha)}$	Density $\rho^{(\alpha)}$ (g cc^{-1})	Young's modulus $E^{(\alpha)}$ (dyn cm^{-2})	Poisson's ratio $\nu^{(\alpha)}$	Yield stress σ_Y (dyn cm^{-2})	Hardening parameter H' (dyn cm^{-2})
1	0.272	1.85	292.0 (10^9)	0.3776	—	—
2	0.728	1.29	82.24 (10^9)	0.357	1.33 (10^9)	11.38 (10^9)

MODEL VALIDATION STUDIES

In this section, validation studies are conducted in an effort to ascertain the simulation capability of the $O(\varepsilon)$ mixture continuum model. The model consists of the equations of motion (33) and (34), the boundary conditions (40) and (41), the initial conditions (42), and the rate-constitutive relations (50)–(52) and (55)–(58). The problems examined include linear and nonlinear wave propagation. In the dynamic response, mixture model predictions were compared with experimental data or "exact" numerical data generated from DYNA2D based upon detailed explicit modeling of fibers and matrix. Material properties of the investigated composite which consists of elastic fibers and an elastoplastic matrix are shown in Table 1.

For elastic harmonic wave propagation, the model was validated by comparing the predicted phase velocity spectra with experimental data (Murakami and Hegemier, 1986). Therefore, the validation of the model was conducted in the time domain. As was noted previously, the validation strategy is to compare mixture model predictions with experimental data or "exact" numerical data generated from DYNA2D based upon detailed explicit modeling of fibers and matrix. For this purpose, an explicit finite element code: HFEC2D (Impelluso, 1990) was developed using four-node quadrilateral elements for the generalized plane strain in the x_1, x_2-plane. The mixture element has six nodal degrees-of-freedom for $U_i^{(\alpha)}$ and S_i^2 ($i = 1, 2$). The element carries the microstructure of the cell at each integration point where the numerical integration of incremental constitutive equations (50) (58) are conducted. For simplicity of notation in the numerical results, dimensional quantities are referred without overbars.

The geometry of the wave-reflect problem is shown in Fig. 3 with meshes for HFEC2D (Fig. 3b) and the detailed DYNA2D (Fig. 3c). A composite half space with free boundary at $x_2 = 0$ was loaded uniformly with respect to x_3 under a plane strain condition in the x_1-direction. For this globally one-dimensional wave phenomenon in the x_2-direction, a column of cells of width $\Delta = 0.0975$ cm, shown in Fig. 3a, is discretized by the mesh shown in Fig. 3c for DYNA2D calculation; for the mixture model only one row of elements shown in Fig. 3b is employed. The following boundary conditions were posed for the DYNA2D

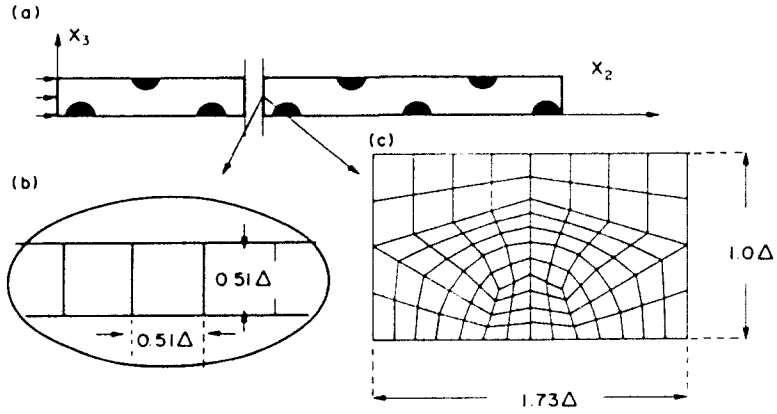

Fig. 3. Geometry of the wave-reflect problem: (a) overview; (b) HFEC2D mesh with dimensions in the x_1, x_2 plane, and with microstructure in the x_2^*, x_3^* plane; (c) DYNA2D mesh with dimensions.

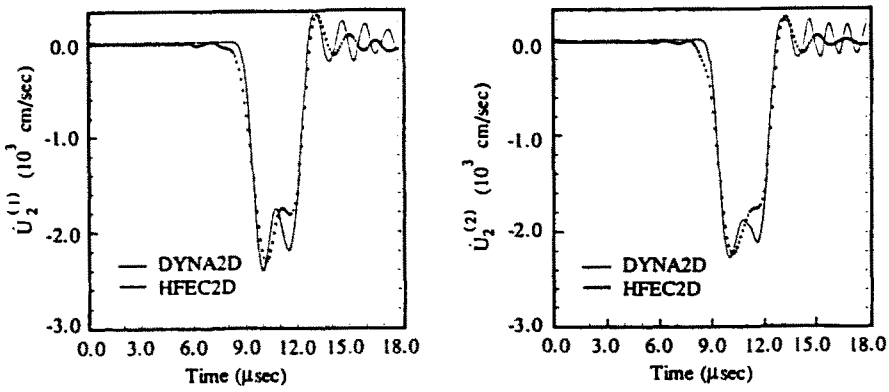

Fig. 4. Time variation of particle velocity for the elastic wave-reflect analysis: (a) fiber, $\dot{U}_2^{(1)}$; (b) matrix, $\dot{U}_2^{(2)}$.

calculation:

$$\sigma_{22} = \sigma_0\{H(t) - H(t-t_0)\}, \quad \sigma_{23} = 0 \quad \text{at } x_2 = 0$$
$$u_3 = \sigma_{23} = 0 \quad \text{at } x_3 = 0, \Delta. \tag{59}$$

For the mixture model, the corresponding boundary data were specified as

$$\sigma_{22}^{(\alpha)} = n^{(\alpha)}\sigma_0\{H(t) - H(t-t_0)\}, \quad \sigma_{12}^{(\alpha)} = \hat{M}_{12} = \hat{M}_{22} = 0 \quad \text{at } x_2 = 0$$
$$U_1^{(\alpha)} = \sigma_{12}^{(\alpha)} = \hat{M}_{11} = \hat{M}_{12} = 0 \quad \text{at } x_1 = 0, \Delta, \tag{60}$$

where $H(t)$ denotes the Heaviside step function, and $t_0 = 3$ μs is the pulse duration.

A load of $\sigma_0 = 1 \times 10^9$ dyn cm^{-2} is applied to induce a purely elastic response in both constituents, while a load of $\sigma_0 = 3 \times 10^9$ dyn cm^{-2} is applied to induce an elastoplastic response in the matrix. The numerical results are shown for observation points located in the 33rd cell. The time variations of fiber particle velocity, at $r = 0$, $\dot{U}_2^{(1)}$ and of matrix particle velocity $\dot{U}_2^{(2)}$ at $r = 1$ and $\theta = 0°$ are shown, respectively in Fig. 4a and b. The corresponding time variations for the elastoplastic case are shown in Fig. 5a and b. Arrival time, peak response and damping are well correlated by the mixture elements. The dispersive behavior is evident and well matched; furthermore, the spreading of the wave pulse to a duration larger than 3 μs is demonstrated in both DYNA2D and HFEC2D.

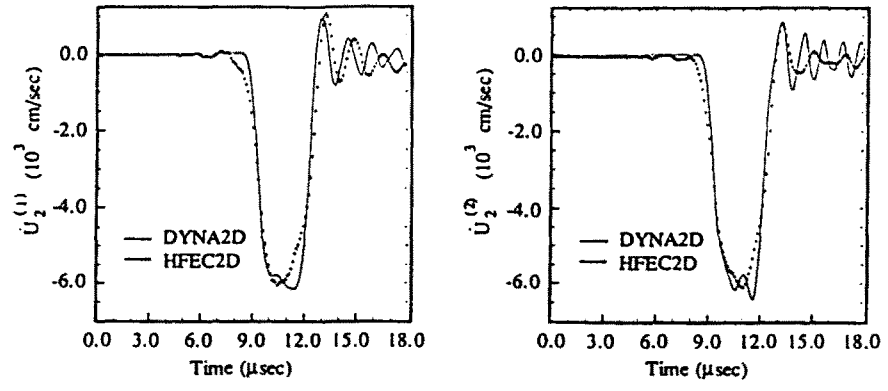

Fig. 5. Time variation of particle velocity for the elastoplastic wave-reflect analysis: (a) fiber, $\dot{U}_2^{(1)}$; (b) matrix, $\dot{U}_2^{(2)}$.

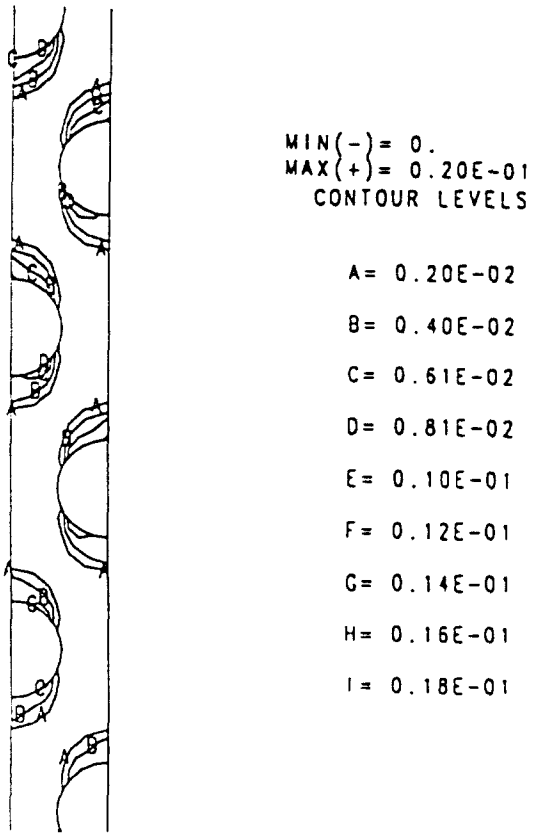

Fig. 6. Effective plastic strain contour obtained from DYNA2D.

Special attention is paid now to the localized plastic deformation in the composite. Figure 6 shows the effective plastic strain contour obtained from DYNA2D; plastic deformation is localized near $\theta = 0^\circ$ and 180°. To examine the capability of the model in predicting those localized effects, the effective stresses at $\theta = 150^\circ$ and 180° both at $r = 0.761$ are shown, respectively, in Fig. 7a and b. From those figures, the localization is modeled accurately by the mixture element. This accuracy is also reflected in the predictions of the effective plastic strain.

In order to further assess the accuracy of the model, the waveguide problem illustrated in Fig. 8 is considered. The load is applied at the boundary $x_1 = 0$ in the fiber axis direction. Hexagonal symmetry, approximated by axisymmetry, allows for an extraction of a cell of radius $\Delta = 0.0975$ cm. First, a comparison is made with a shock tube test conducted by the

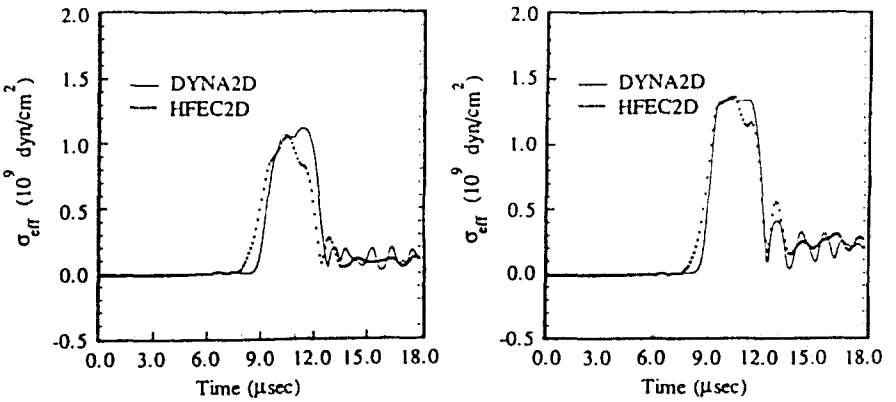

Fig. 7. Time variation of effective stress in the matrix domain for the elastoplastic wave-reflect analysis: (a) $\theta = 150^\circ$; $r = 0.761$; (b) $\theta = 180^\circ$; $r = 0.761$.

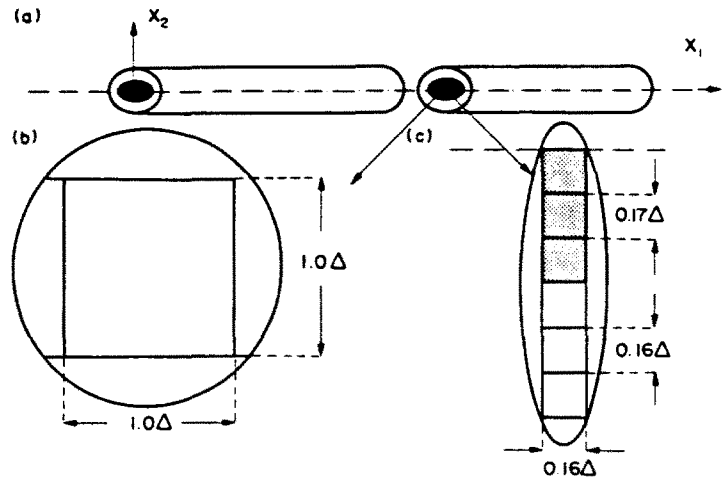

Fig. 8. Geometry of the wave-guide problem: (a) overview; (b) HFEC2D mesh with dimensions in the x_1, x_2 plane, and with microstructure in the x_1^*, x_2^* plane; (c) DYNA2D mesh with dimensions.

Aerospace Corporation and reported by Hegemier *et al.* (1973). The composite is subjected to a step pressure loading of 4.826×10^5 Pa. The results of the model are obtained by using 100 elements. The comparison of the rear surface velocities on a specimen 6.33 mm thick is shown in Fig. 9. In the above experiment the nonlinear effect was negligible.

Numerical experiments were conducted to test the model's capability for predicting elastoplastic wave propagation. The following boundary conditions with respect to the cylindrical coordinate system were posed for the DYNA2D calculation; x_1 and x_2 are, respectively the axial and radial coordinates:

$$\sigma_{11} = \sigma_0\{H(t) - H(t-t_0)\}, \quad \sigma_{12} = 0 \quad \text{at } x_1 = 0$$
$$u_2 = \sigma_{12} = 0 \quad \text{at } x_2 = 0, \Delta. \tag{61}$$

For the mixture model, the corresponding boundary data were specified as

$$\sigma_{11}^{(\alpha a)} = n^{(\alpha)}\sigma_0\{H(t) - H(t-t_0)\}, \quad \sigma_{12}^{(\alpha a)} = \hat{M}_{11}^{2} = \hat{M}_{12}^{2} = 0 \quad \text{at } x_1 = 0$$
$$U_2^{(\alpha)} = \sigma_{12}^{(\alpha a)} = \hat{M}_{12}^{2} = \hat{M}_{22}^{2} = 0 \quad \text{at } x_2 = 0, 0.51\Delta. \tag{62}$$

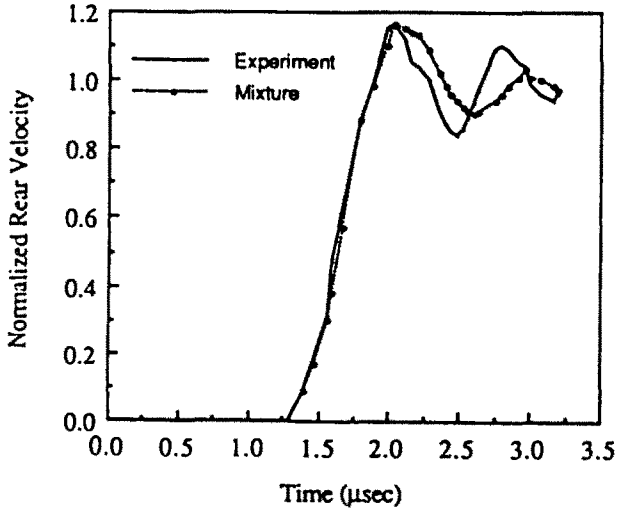

Fig. 9. Time variation of normalized rear velocity.

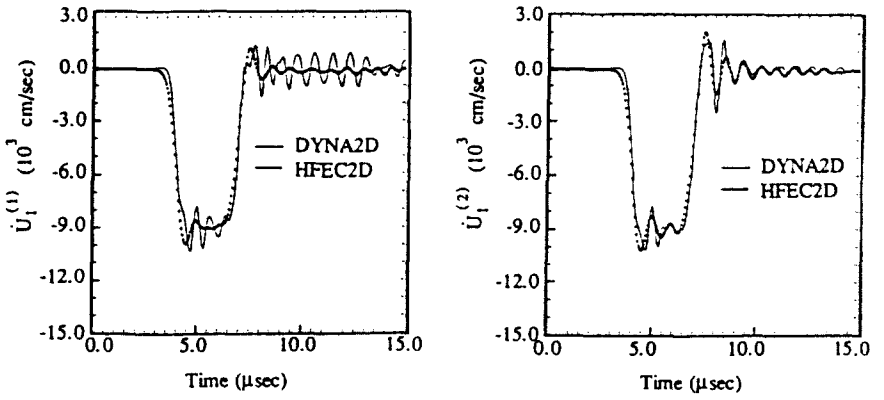

Fig. 10. Time variation of particle velocity for the elastoplastic waveguide analysis: (a) fiber, $\dot{U}_1^{(1)}$; (b) matrix, $\dot{U}_1^{(2)}$.

A pulse load $\sigma_0 = 5.0 \times 10^9$ dyn cm^{-2} of duration $t_0 = 3$ μs was applied. Axial velocities at $x_1 = 43.5\Delta$ were plotted in Fig. 10a for fiber and in Fig. 10b for matrix.

The above comparisons with the detailed FE analyses indicate the cost efficiency of the mixture element due to the coarseness of the mesh; the mixture code, HFEC2D, runs at least an order of magnitude faster than the detailed finite element computation.

CONCLUDING REMARKS

The construction of a higher-order mixture description of fiber-reinforced composites has been demonstrated for the case of material nonlinearities. For simplicity of presentation, composites with a hexagonal array of fibers and elastoplastic matrix were considered. The methodology is based upon an asymptotic homogenization method and yields the equations of motion, the appropriate initial and boundary conditions, and a set of consistent rate-constitutive relations. For transient response a finite element wave code was developed for the mixture model to solve linear and nonlinear problems; results using this code were compared with those from DYNA2D in which a fine mesh was utilized to explicitly model the microstructure of the composite. These comparisons reveal that the mixture model is capable of furnishing an accurate and economical description of complex wave phenomena. In the foregoing analyses the importance of wave dispersion and attenuation effects was confirmed for nonlinear as well as linear composite responses.

Acknowledgements—The research was supported by the Office of Naval Research (ONR) under Contract N00014-86-K-0468 and by the Defense Advanced Research Projects Agency (DARPA) under Contracts N00014-88-C-2029 and N00014-88-C-0740 issued by the Office of Naval Research.

REFERENCES

Aboudi, J. (1981). Generalized effective stiffness theory for the modeling of fiber-reinforced composites. *Int. J. Solids Structures* **17**, 1005–1018.

Aboudi, J. (1982). A continuum theory for fiber-reinforced elastic–viscoplastic composites. *Int. J. Engng Sci.* **20**, 605–621.

Aboudi, J. (1985). The effective thermomechanical behavior of inelastic fiber-reinforced materials. *Int. J. Engng Sci.* **23**, 773–787.

Achenbach, J. D. (1975). *A Theory of Elasticity with Microstructure for Directionally Reinforced Composites*. Springer, New York.

Achenbach, J. D. (1976). Generalized continuum theories for directionally reinforced solids. *Arch. Mech.* **28**, 257–278.

Achenbach, J. D. and Herrmann, G. (1968). Dispersion of free harmonic waves in fiber-reinforced composites. *AIAA Jl* **6**, 1832–1836.

Babuška, I. (1976). Solution of interface problems by homogenization. *SIAM Jl Appl. Math.* **7**, Part I, 603–634; Part II, 635–645.

Bartholomew, R. A. and Torvick, P. J. (1972). Elastic wave propagation in filamentary composite materials. *Int. J. Solids Structures* **8**, 1389–1405.

Bensoussan, A., Lions, J. L. and Papanicolaou, G. (1978). *Asymptotic Analysis for Periodic Structures*. North-Holland, Amsterdam.
Brillouin, L. (1946). *Wave Propagation in Periodic Structures*. Dover, New York.
Choi, D. S. and Bedford, A. (1973). Transient pulse propagation in a fiber-reinforced material. *J. Acoust. Soc. Amer.* **54**, 676–684.
Hallquist, J. O. (1982). User's manual for DYNA2D—an explicit two-dimensional hydrodynamic finite element code with interactive rezoning. Report UCID-18756, University of California, Lawrence Livermore National Laboratory.
Hegemier, G. A. and Gurtman, G. A. (1974). Finite-amplitude elastic–plastic wave propagation in fiber-reinforced composites. *J. Appl. Phys.* **45**, 4245–4261.
Hegemier, G. A., Gurtmann, G. A. and Nayfeh, A. H. (1973). A continuum mixture theory of wave propagation in laminated and fiber-reinforced composites. *Int. J. Solids Structures* **9**, 395–414.
Hegemier, G. A., Murakami, H. and Maewal, A. (1979). On construction of mixture theories for composite materials by the method of multi-variable asymptotic expansion. *Proc. Third Int. Symp. on Continuum Models of Discrete Systems*, Freudenstadt, Germany, pp. 423–441.
Hlaváček, M. (1975). A continuum theory for fiber-reinforced composites. *Int. J. Solids Structures* **11**, 199–217.
Hughes, T. J. R. (1987). *The Finite Element Method, Linear Static and Dynamic Finite Element Analysis*. Prentice-Hall, Englewood Cliffs, New Jersey.
Impelluso, T. J. (1990). A finite element implementation of a high-order homogenization theory. Ph.D. thesis, University of California, San Diego.
Kittel, C. (1971). *Introduction to Solid State Physics*. Wiley, New York.
Kohn, W., Krumhansl, J. A. and Lee, E. H. (1972). Variational methods for dispersion relations and elastic properties of composite materials. *J. Appl. Mech.* **39**, 327–336.
Lene, F. and Leguillon, D. (1982). Homogenized constitutive law for a partially cohesive composite material. *Int. J. Solids Structures* **18**, 443–458.
Marsden, J. E. and Hughes, T. J. R. (1983). *Mathematical Foundations of Elasticity*. Prentice-Hall, Englewood Cliffs, New Jersey.
Martin, S. E., Bedford, A. and Stern, M. (1971). Steady state wave propagation in fiber reinforced elastic materials. *Proc. 12th Midwestern Mechanics Conf., Developments in Mechanics* **6**, 515–528.
Murakami, H. (1991). Surface wave in a half-space with a single-set of periodic joints. *J. Geophys. Res.* **96**(B3), 4173–4186.
Murakami, H. and Hegemier, G. A. (1986). A mixture model for unidirectionally fiber-reinforced composites. *J. Appl. Mech.* **53**, 765–773.
Murakami, H., Maewal, A. and Hegemier, G. A. (1979). Mixture theory for longitudinal wave propagation in unidirectional composites with cylindrical fibers of arbitrary cross-section—I. Formulation. *Int. J. Solids Structures* **15**, 325–334.
Murakami, H., Maewal, A. and Hegemier, G. A. (1981). A mixture theory with a director for linear elastodynamics of periodically laminated media. *Int. J. Solids Structures* **17**, 155–173.
Nayfeh, A. H. (1977). Thermomechanically induced interfacial stresses in fibrous composites. *Fiber Sci. Technol.* **10**, 195–209.
Nayfeh, A. H., Crane, R. L. and Hoppe, W. L. (1984). Reflection of acoustic waves from water/composite interfaces. *J. Appl. Phys.* **55**, 685–689.
Reissner, E. (1984). On a certain mixed variational theorem and a proposed application. *Int. J. Numer. Meth. Engng* **20**, 1366–1368.
Reissner, E. (1986). On a mixed variational theorem and on shear deformable plate theory. *Int. J. Numer. Meth. Engng* **23**, 193–198.
Sanchez-Palencia, E. (1980). *Non-Homogeneous Media and Vibration Theory*. Lecture Notes in Physics, 127. Springer, Berlin.
Tartar, L. (1977). Cours Peccot. College de France.

APPENDIX. DEFINITIONS OF $[E_{ij}]$ IN EQUATION (43)

It is computationally advantageous to rewrite eqn (10) in terms of the elastoplastic compliance matrix $\mathbf{D} = \mathbf{C}^{-1}$. For a von Mises yield criterion and associated flow rule with linear strain hardening, $\mathbf{D}^{(\alpha)(\mathrm{ep})}$ may be expressed as

$$\mathbf{D}^{(\alpha)(\mathrm{ep})} = \mathbf{D}^{(\alpha)} + \frac{9}{4\bar{\sigma}^{(\alpha)2}H'^{(\alpha)}}\mathbf{s}^{(\alpha)}\mathbf{s}^{(\alpha)\mathrm{T}}. \tag{A1}$$

In eqn (A1), H' is the strain hardening parameter, $\mathbf{s}\ (=\boldsymbol{\sigma}-\mathrm{tr}\,\boldsymbol{\sigma}.\boldsymbol{\delta})$ is the deviatoric stress, and $\bar{\sigma}\ (=\sqrt{3\mathbf{s}:\mathbf{s}/2})$ is the von Mises effective stress.

Rewriting the rate compliance relation by using a 6×6 matrix $[D]$ for $\mathbf{D}$, one finds

$$E_{11}^{(\alpha)} = \frac{1}{D_{11}^{(\alpha)(\mathrm{ep})}},\quad [E_{1j}^{(\alpha)}] = \frac{1}{D_{11}^{(\alpha)(\mathrm{ep})}}[D_{12}\ \ D_{13}\ \ D_{14}\ \ D_{15}\ \ D_{16}]^{(\alpha)(\mathrm{ep})},\quad [E_{ij}^{(\alpha)}] = D_{ij}^{(\alpha)(\mathrm{ep})} - \left(\frac{D_{1i}\ D_{1j}}{D_{11}}\right)^{(\alpha)(\mathrm{ep})},\quad i,j = 2\ 6. \tag{A2}$$